Cell Reports, Volume *23*

Supplemental Information

Inhibition of Lysosome Membrane Recycling Causes Accumulation of Gangliosides that Contribute to Neurodegeneration

Maxime Boutry, Julien Branchu, Céline Lustremant, Claire Pujol, Julie Pernelle, Raphaël Matusiak, Alexandre Seyer, Marion Poirel, Emeline Chu-Van, Alexandre Pierga, Kostantin Dobrenis, Jean-Philippe Puech, Catherine Caillaud, Alexandra Durr, Alexis Brice, Benoit Colsch, Fanny Mochel, Khalid Hamid El Hachimi, Giovanni Stevanin, and Frédéric Darios

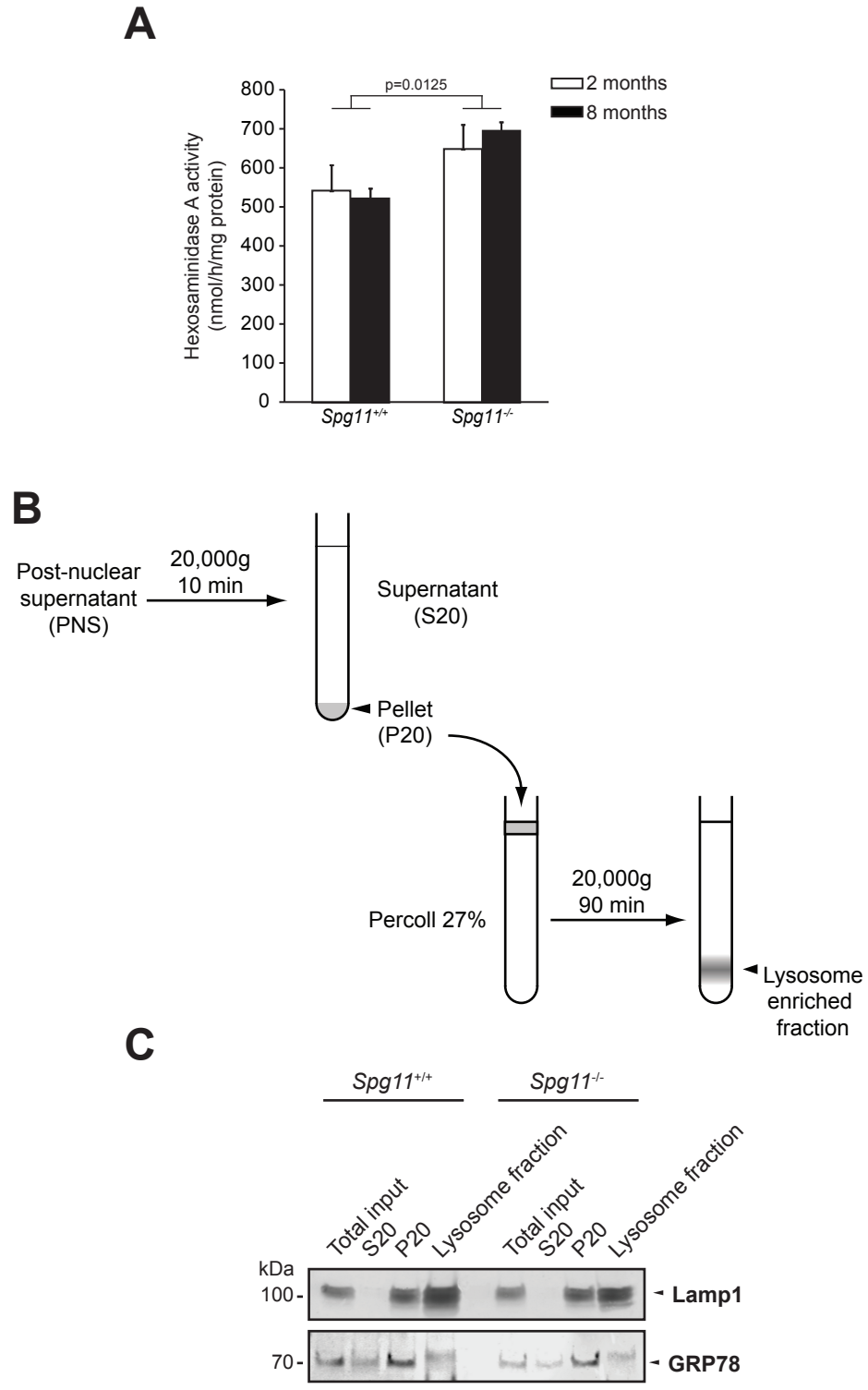

Figure S1: Investigation of lysosome functions in *Spg11*$^{+/+}$ and *Spg11*$^{-/-}$ mouse brain.
Related to Figure 1 and Table 1.
(**A**) Hexosaminidase A activity monitored in cortex of *Spg11*$^{+/+}$ and *Spg11*$^{-/-}$ mice. N=5. Two-way ANOVA. (**B**) Scheme showing the procedure used to purify fractions enriched in lysosomes. (**C**) Western blot analysis of whole brain lysate, fractions S20, P20, and the lysosome-enriched fraction obtained from *Spg11*$^{+/+}$ and *Spg11*$^{-/-}$ mouse brain.

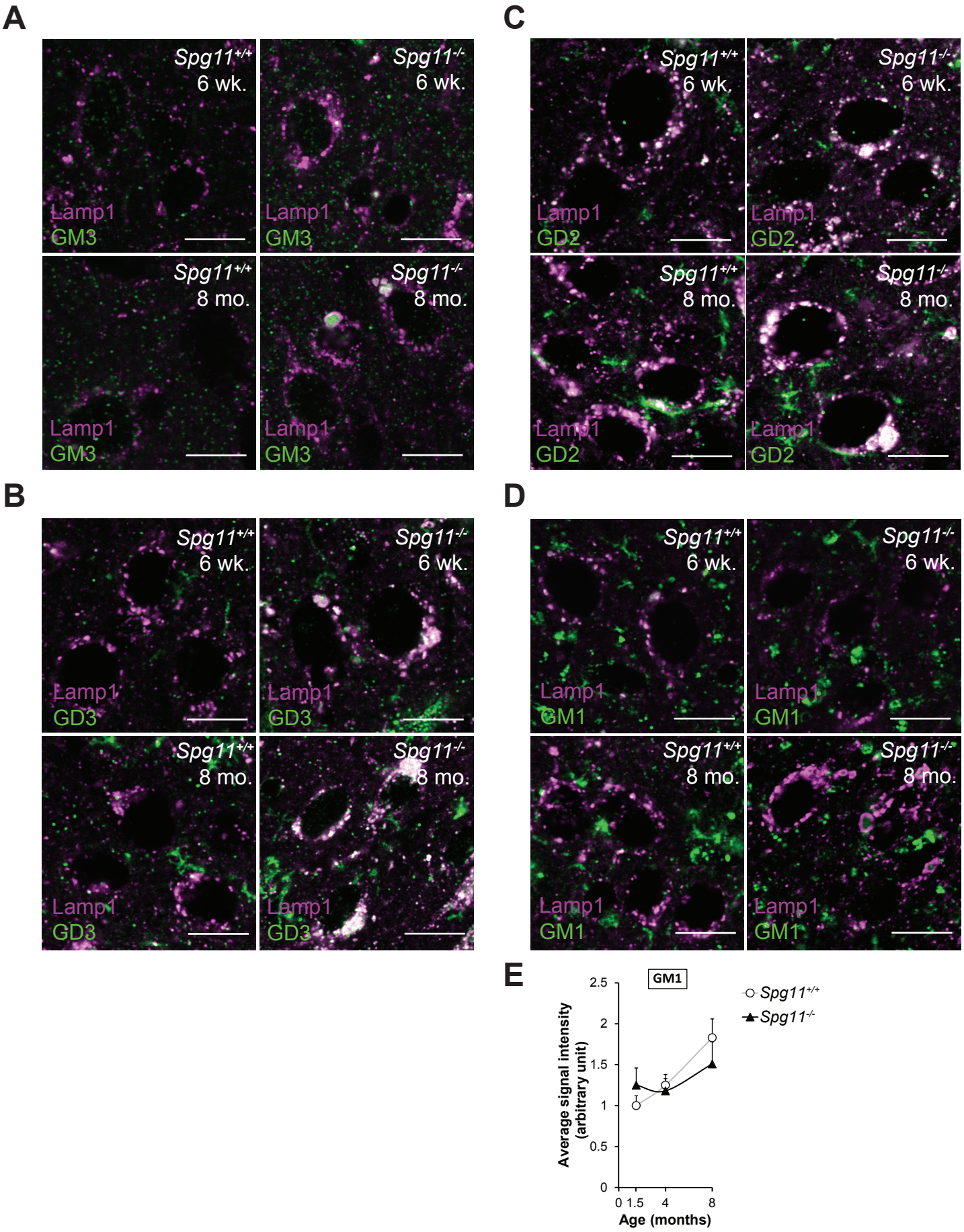

Figure S2. Spatacsin loss promotes lysosomal accumulation of gangliosides in neurons of the cortex. Related to Figure 1.

(**A-D**) Immunostaining of Lamp1 (magenta) and GM3 (**A**), GD3 (**B**), GD2 (**C**) and GM1 (**D**) in Spg11$^{+/+}$ and Spg11$^{-/-}$ cortical motor neurons of the layer V of the motor cortex from six-week-old (6wk.) and eight-month-old (8 mo.) mice. Scale bars: 10 µm. (**E**) Quantification of the mean of the GM1 immunostaining intensity per neuron. Quantification was performed in neurons of the layer V of motor cortex that were detected by their large soma. The graph shows the mean ± SEM values. N = 10-15 neurons quantified in five cortex slices of 5 five independent mice.

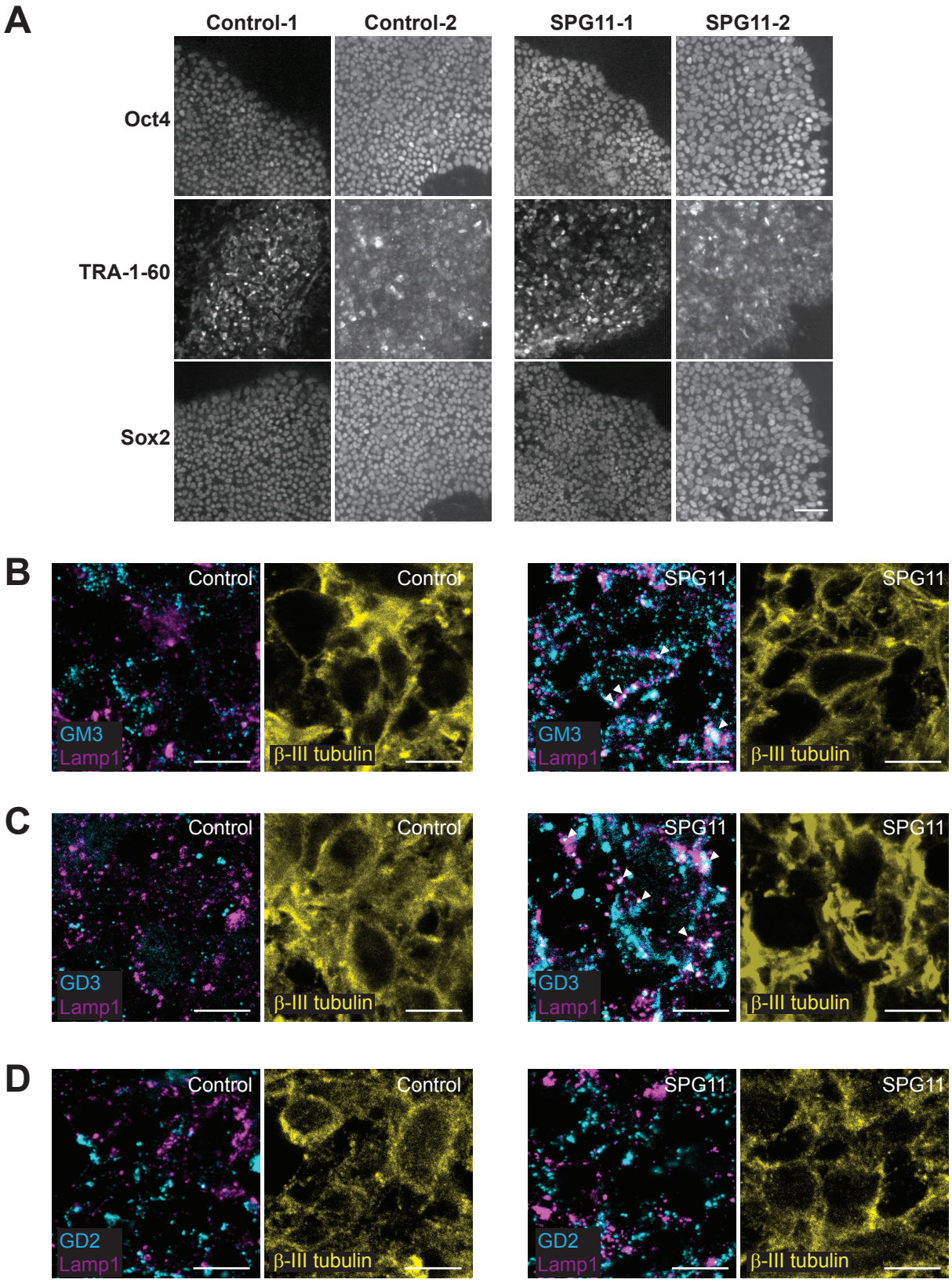

Figure S3. Spatacsin loss promotes lysosomal accumulation of GM3 and GD3 gangliosides in neurons derived from SPG11 patients. Related to Figure 2.

(**A**) Immunostaining of iPS cells with pluripotency markers. Scale bar: 20µm.

(**B-D**) Immunostaing of Lamp1 (magenta) and GM3 (B), GD3 (C) or GD2 (D) in the neuronal layer of organoids derived from healthy subjects (Control) or SPG11 patients. βIII-tubulin (yellow) shows the neuronal identity of the cells that were analyzed. Confocal microscopy images showing the accumulation of GM3- and GD3-positive staining in lysosomes labelled by Lamp1 staining of organoids derived from SPG11 patients (arrowheads). Scale bars: 10 µm.

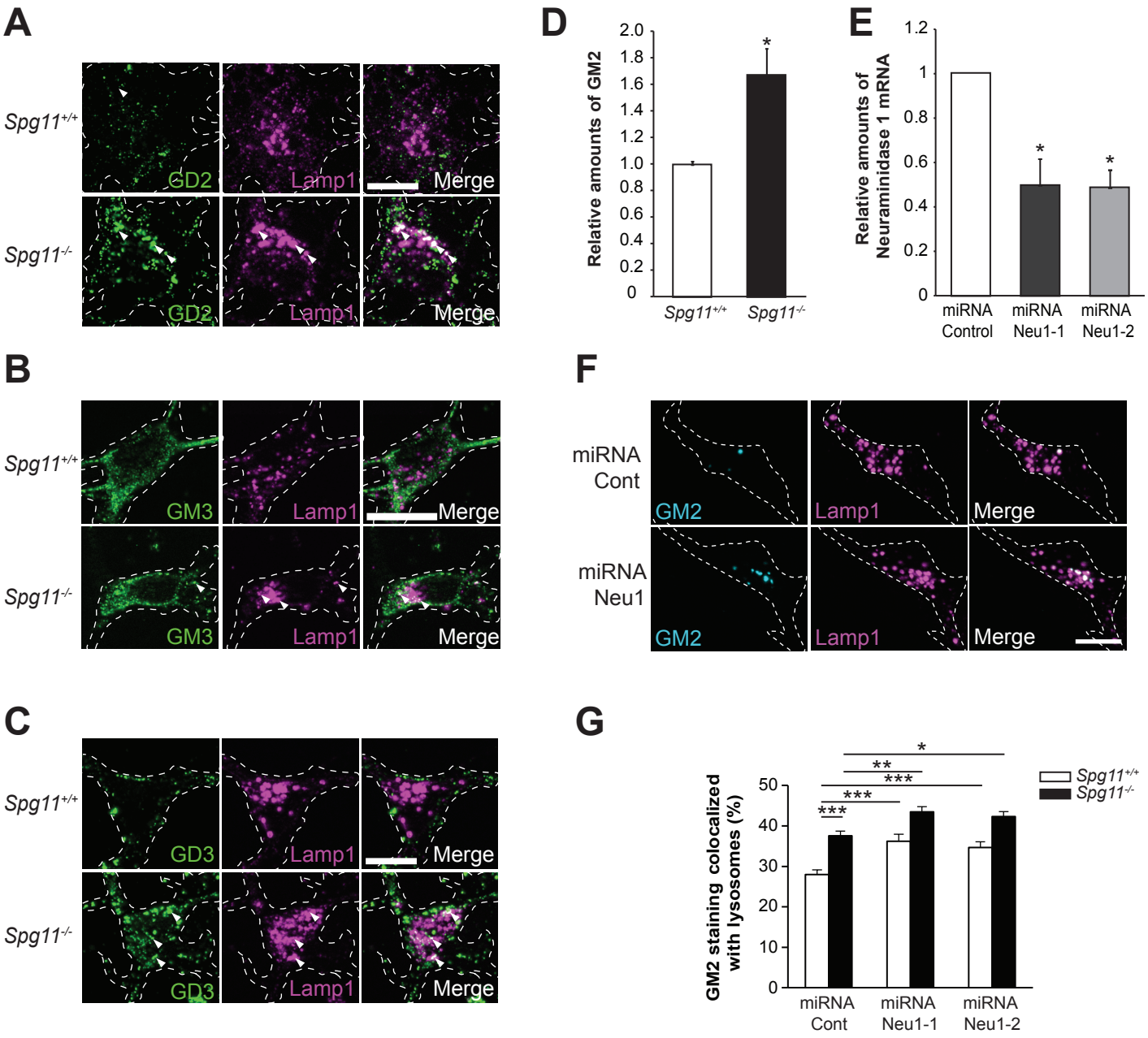

Figure S4: Downregulation of Neu1 increases ganglioside levels in lysosomes in cultured wild-type neurons. Related to Figure 3

(**A-C**) Immunostaining of Lamp1 (magenta) and GD2 (**A**), GM3 (**B**) and GD3 (**C**) in *Spg11*$^{+/+}$ and *Spg11*$^{-/-}$ neurons cultured for six days *in vitro*. Confocal microscopy images showing the accumulation of gangliosides in lysosomes labeled by Lamp1 staining. Scale bars: 10 µm. (**D**) Relative amount of GM2 monitored by lipidomic analysis in *Spg11*$^{+/+}$ and *Spg11*$^{-/-}$ neurons cultured for six days *in vitro*. N = 5 and 6 neuronal preparations for *Spg11*$^{+/+}$ and *Spg11*$^{-/-}$ neurons, respectively. Welsh's t-test, p=0.026. (**E**) qRT-PCR showing the decrease in Neu1 mRNA in mouse NIH-3T3 cells transfected with the vectors expressing two different miRNAs targeting Neu1 or a control vector. N = 4. Kruskal-Wallis test, *p < 0.05. (**F**) Effect of Neu1 downregulation on staining with antibodies directed against GM2 (cyan) and Lamp1 (magenta). Note the increase in the number of lysosomes labeled with GM2 after downregulation of Neu1. Scale bar: 10 µm. (**G**) Quantification of the proportion of GM2 staining that is localized to lysosomes in neurons transfected with vectors expressing two independent miRNAs directed against Neu1. The graph shows the mean ± SEM values. N = 49-61 neurons quantified in three independent neuron preparations. Two-way ANOVA, followed by Holm-Sidak post-hoc test; *p < 0.05; **p < 0.01; ***p < 0.001.

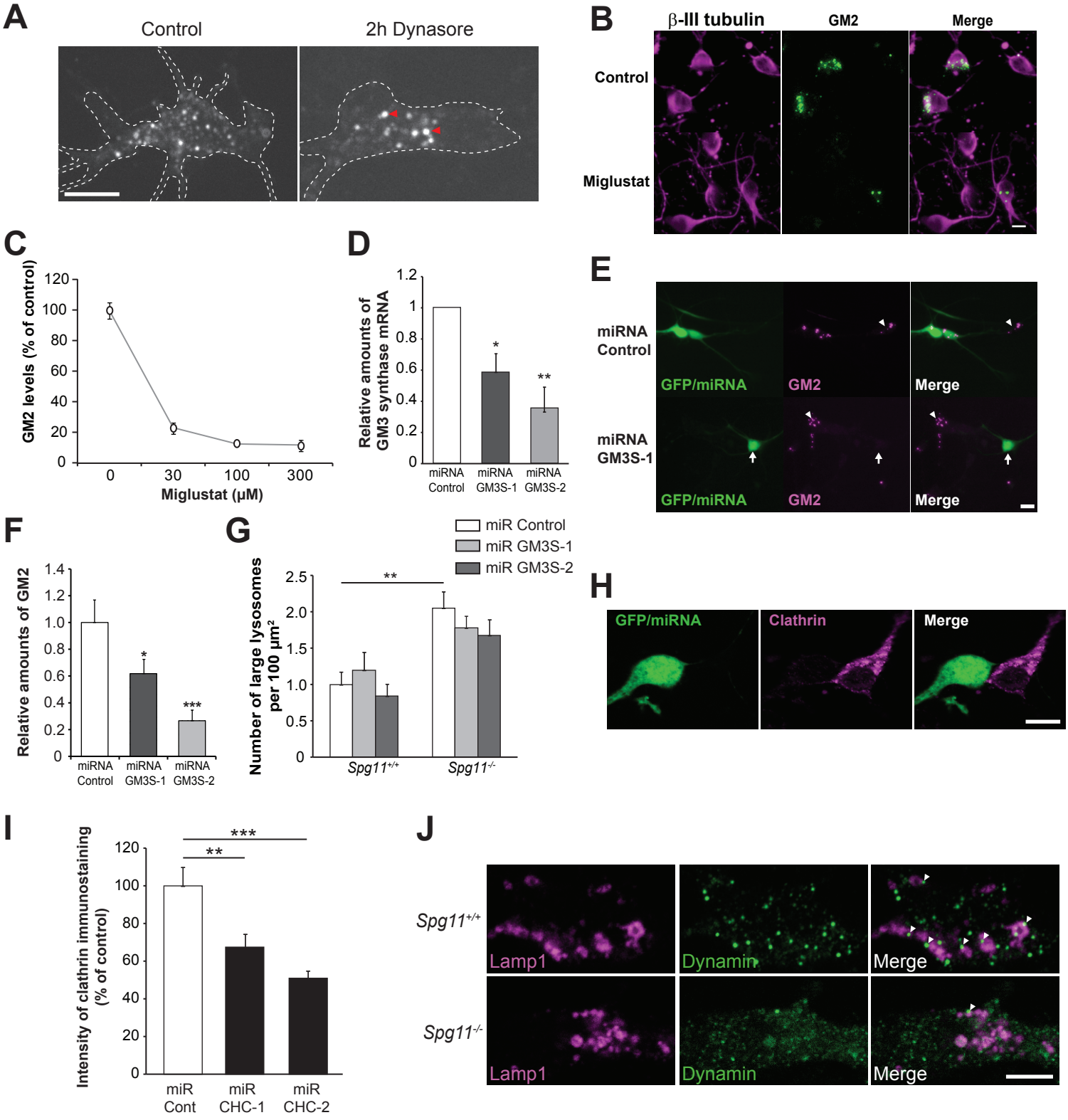

Figure S5. Inhibition of ganglioside synthesis decreases ganglioside levels in cultured neurons. Related to Figure 4.
(**A**) Iive imaging of neurons expressing Lamp1-mcherry, treated with vehicle or Dynasore (40μM) for 2 hours. Arrowheads point to lysosomes with a diameter larger than 1μm. Scale bar: 10μm. **(B)** β–III tubulin (magenta, neuronal marker) and GM2 immunostaining (green) of primary cultures of cortical neurons treated or not with miglustat (100μM) for six days *in vitro*. Scale bar: 10μm. **(C)** Quantification of the fluorescence intensity of GM2 immunostaining of primary cultures of cortical neurons cultured for six days *in vitro* with various concentrations of miglustat. The graph shows the mean ± SEM values. N = 3 independent experiments. **(D)** qRT-PCR showing the decrease in GM3 synthase mRNA in mouse NIH-3T3 cells transfected with the vectors expressing two different miRNAs targeting the GM3 synthase or a control vector. N = 3. Kruskal-Wallis test, *p = 0.048; **p=0.003. **(E)** GM2 immunostaining (magenta) of cells transfected with vector expressing GFP and miRNA to downregulate GM3 synthase. The arrow indicates a cell transfected with miRNA against GM3 synthase, showing weak GM2 immunostaining. Arrowheads indicate non-transfected cells. Scale bar: 10μm. **(F)** Quantification of the fluorescence intensity of GM2 in neurons transfected with vectors

expressing control miRNA or two different miRNA against GM3 synthase. N = 45-63 neurons in two independent experiments. One-way ANOVA, followed by Holm-Sidak post-hoc test; *p=0.03, ***p<0.001. **(G)** Quantification of the number of lysosomes with a diameter larger than 1µm in *Spg11*$^{+/+}$ and *Spg11*$^{-/-}$ neurons expressing control miRNA or miRNA downregulating GM3 synthase. The graph shows the mean ± SEM values. N = 14-33 neurons quantified in three independent neuron preparations. One-way ANOVA, followed by Holm-Sidak post-hoc test; **p=0.0024. **(H)** Clathrin heavy chain immunostaining of neurons transfected with vector expressing GFP and miRNA to downregulate clathrin heavy chain. **(I)** Quantificationof the intensity of clathrin immunostaining in neurons transfected with vectors expressing control miRNA or miRNA downregulating clathrin heavy chain. The graph shows the mean ± SEM values. N =44-53 neurons quantified in two independent neuron preparations. One-way ANOVA, followed by Holm-Sidak post-hoc test; **p=0.0016, ***p<0.001. **(J)** Lamp1 (magenta) and dynamin (green) immunostaining of *Spg11*$^{+/+}$ and *Spg11*$^{-/-}$ neurons showing decreased recruitment of dynamin to lysosomes in *Spg11*$^{-/-}$ neurons. Arrowheads point recruitment of dynamin at the edge of lysosomes. Scale bar: 5µm.

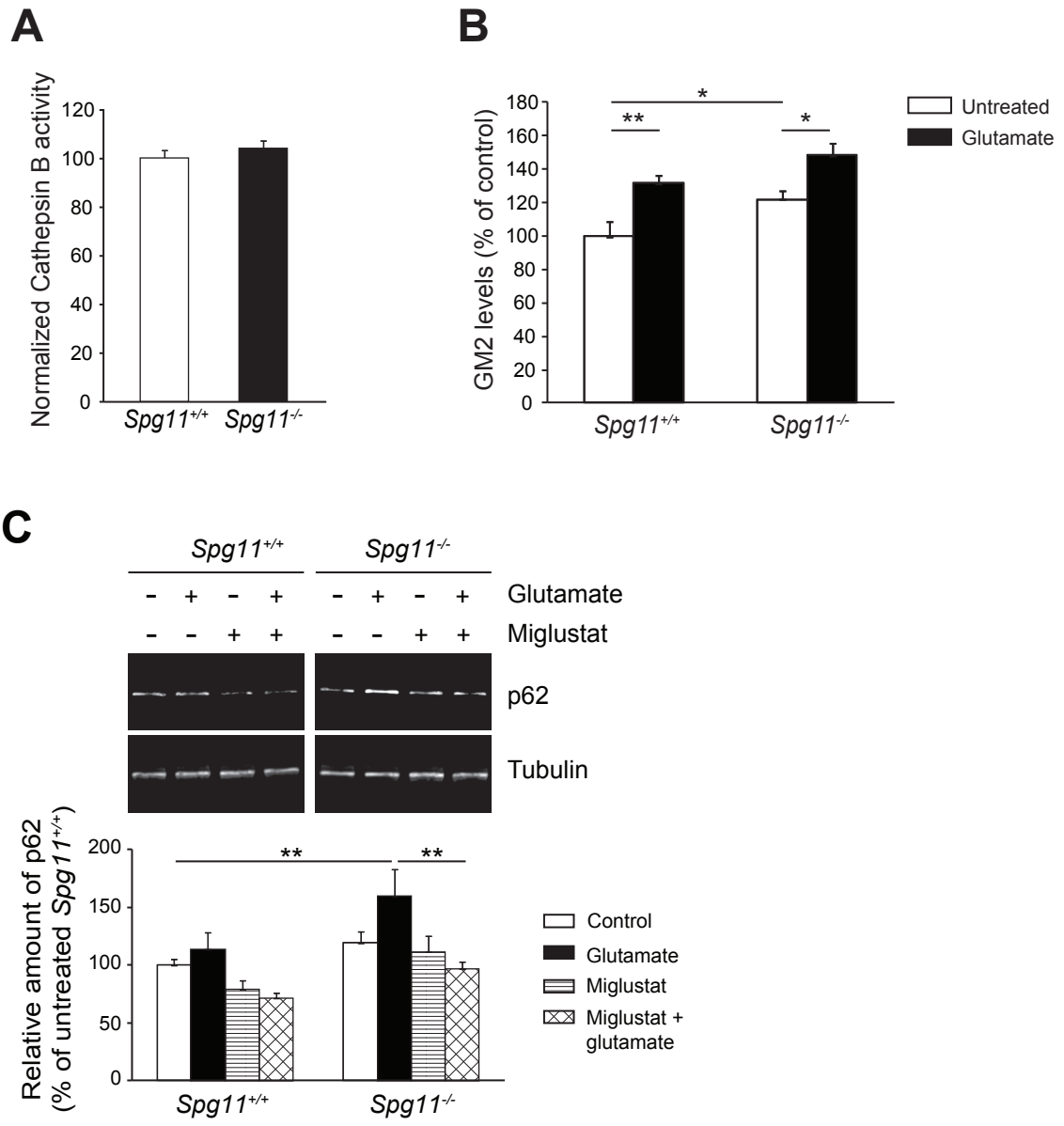

Figure S6: Glutamate treatment increases GM2 levels in *Spg11*$^{+/+}$ and *Spg11*$^{-/-}$ neurons.
Related to Figure 5.

(**A**) Normalized catalytic activity of cathepsin B monitored with the Magic Red Cathepsin B Assay Kit in primary cultures of *Spg11*$^{+/+}$ and *Spg11*$^{-/-}$ neurons after six days in vitro. N = 3 independent experiments performed in quadruplicate. (**B**) Quantification of fluorescence intensity of GM2 immunostaining of primary cultures of *Spg11*$^{+/+}$ and *Spg11*$^{-/-}$ cortical neurons that were treated for 24 hours with 200µM glutamate. The graph shows the mean ± SEM values. N = 7-10 independent neuron preparations. One-way ANOVA, followed by Holm-Sidak post-hoc test;* $p<0.05$, ** $p<0.01$. (**C**) Western blot analysis of p62 levels in *Spg11*$^{+/+}$ and *Spg11*$^{-/-}$ cortical neurons treated or not with miglustat (100 µM). Neurons were incubated with glutamate (200 µM) for 24 hours. Graph showing the quantification of the relative amount of p62 normalized to tubulin in *Spg11*$^{+/+}$ and *Spg11*$^{-/-}$ cortical neurons treated with miglustat or glutamate. N = 5-9 independent experiments. One-way ANOVA, followed by Holm-Sidak post-hoc test; **$p < 0.01$.

	Spg11$^{+/+}$	*Spg11*$^{-/-}$	Fold change
Fatty Acyls	**N=8**	**N=8**	
Total Free fatty acids (FA)	**87.31 ± 5.12**	**61.74 ± 4.54***	**0.71**
Glycerolipids			
Total Diacylglycerols (DG)	25.44 ± 2.31	23.68 ± 2.04	0.93
Total Triacylglycerols (TG)	39.92 ± 3.79	33.13 ± 4.22	0.83
Total Cardiolipines (CL)	11.01 ± 0.92	10.39 ± 0.61	0.94
Glycerophospholipids			
Total Lyso-Glycerophosphocholines (LPC)	**60.62 ± 4.32**	**43.46 ± 3.02***	**0.72**
Total Lyso-Glycerophosphoethanolamines (LPE)	**4.96 ± 0.36**	**3.66 ± 0.23***	**0.74**
Total Lyso-Glycerophosphoinositols (LPI)	**5.40 ± 0.28**	**3.51 ± 0.36***	**0.65**
Total Lyso-Glycerophosphoserines (LPS)	**5.31 ± 0.27**	**3.54 ± 0.30***	**0.67**
Total Glycerophosphocholines (PC)	15685.80 ± 1134.25	14329.06 ± 819.96	0.91
Total Glycerophosphoethanolamines (PE)	2668.36 ± 124.22	2491.88 ± 80.92	0.93
Total Glycerophosphoglycerols (PG)	38.18 ± 2.32	36.38 ± 1.38	0.95
Total Glycerophosphoinositols (PI)	603.44 ± 25.71	552.21 ± 23.50	0.92
Total Glycerophosphoserines (PS)	512.32 ± 26.65	472.93 ± 35.49	0.92
Sphingolipids			
Total Ceramides	**55.41 ± 5.44**	**37.66 ± 1.98***	**0.68**
Total Hexosylceramides	67.68 ± 7.19	60.37 ± 8.78	0.89
Total Gangliosides GM1	13.34 ± 1.08	10.68 ± 0.82	0.80
Total Gangliosides GM2	**0.39 ± 0.04**	**0.58 ± 0.05***	**1.49**
Total Gangliosides GM3	1.05 ± 0.09	1.11 ± 0.08	1.06
Total Gangliosides GD1	76.04 ± 4.83	61.41 ± 3.27	0.81
Total Sphingomyelins	548.17 ± 35.66	541.73 ± 23.91	0.99
Total Sulfoglycosphingolipids	576.35 ± 57.57	501.79 ± 65.14	0.87
Sterol Lipids			
Total Steryl esters	0.86 ± 0.10	0.79 ± 0.08	0.92
Cholesterol	61.61 ± 2.04	58.08 ± 1.82	0.94

Table S1: Relative amounts of various classes of lipids in the cortex of eight-month-old *Spg11*$^{+/+}$ and *Spg11*$^{-/-}$ mice. Related to Figure 1

Arbitrary units, normalized to tissue weight.*$p < 0.05$, T-test with Benjamini-Hochberg procedure to correct for multiple testing. Significant differences are highlighted in bold.

Supplemental Experimental Procedures

Antibodies and Chemicals

Miglustat was obtained from Tocris and dynasore was purchased from Abcam. Antibodies used in the study were: rat anti-Lamp1 (Clone 1D4B, Development Study Hybridoma Bank, University of Iowa), mouse anti-Lamp1 (clone H5G11; Santa Cruz Biotechnologies), mouse anti-GRP78 (BD Biosciences), mouse anti-p62 (Abcam), mouse-anti-clathrin (clone X-22, Abcam for immunocytochemistry; clone 23, BD Biosciences for western blotting), rabbit anti-Pax-6 (Covance), mouse anti-βIII-tubulin (Tuj1; Eurogentec), rabbit anti-sox2 (Millipore), mouse anti-oct4 (Santa Cruz biotechnology), mouse anti-Tra1-60 (Millipore), mouse anti-GM2 (hybridoma supernatant produced in-house) (Dobrenis et al., 1992; Natoli et al., 1986), mouse anti-GM3 (Cosmo Bio), mouse anti-GD2 (Millipore), and mouse anti-GD3 (Invitrogen), rabbit anti-dynamin1 (Abcam), mouse anti-dynamin (BD biosciences). For immunoblotting, the secondary antibodies were conjugated to either fluorochromes (IR-dye 800 or IR-dye 680; LI-COR) for detection with the Odyssey CLX infrared imaging system (Licor), or to horseradish peroxidase (Jackson Immunoresearch) for detection with the Supersignal West Pico Chemiluminescent Substrate (Pierce). Secondary antibodies used for immunofluorescence were purchased from Life Technologies.

Lipidomic analysis

Eight month-old *Spg11*$^{-/-}$ and *Spg11*$^{+/+}$ mice were killed by CO_2 and the cerebral cortices were immediately dissected and frozen in isopentane. Samples were extracted according to a modified Folch method (Folch et al., 1957). Briefly, 10 mg of cortex was added to 190 µL of chloroform/methanol 2:1 (v/v). Samples were vortexed for 60 s and then sonicated for 30 s using a sonication probe. Extraction was performed after 2 h at 4°C with mixing. In addition, 40 µL of ultra-pure water was added and samples were vortexed for 60 s before centrifugation at 10 000 rpm for 10 min at 4°C. The upper phase (aqueous phase), containing ganglioside species and several lysophospholipids, was transferred into a glass tube and then dried under a stream of nitrogen. The interphase which consists on a protein disk was discarded and the lower rich-lipid phase (organic phase) was pooled with the dried upper phase. Samples were then reconstituted with 200 µL of chloroform/methanol 2:1 (v/v), vortexed for 30 s, sonicated for 60 s, and diluted 1/100 in MeOH/IPA/H2O 65:35:5 (v/v/v) before injection.

All samples were processed and analyzed as described previously (Seyer et al., 2016). After liquid chromatography-high-resolution mass spectrometry analysis, samples were re-injected for higher energy collisional dissociation (HCD) tandem mass spectrometry experiments (MS/MS) in the negative ion mode, with the instrument set in the targeted mode, using inclusion lists. The isolation width was set to *m/z* 0.4, the normalized collision energy was 26%, and mass resolution was set to 17,500 FWHM at *m/z* 200. HCD mass spectra were inspected manually to confirm the identity of the ganglioside species. The relative amount of each lipid was quantified as the area of its chromatographic peak, and it was normalized to the exact weight of each cortex to take into account the difference of weight between cortices of *Spg11*$^{-/-}$ and *Spg11*$^{+/+}$ neurons.

Lysosome fractions

Lysosome-enriched fractions were purified from whole brains of eight-month old animals following the self-generated Percoll gradient protocol described previously (Graham, 2001) (Fig S1). At the end of the protocol, the lysosome-enriched fractions were washed once in PBS and the protein quantified by the BCA kit (Pierce). Western blots were performed as described previously (Esteves et al., 2014). Quantifications of band intensities on western blot was performed with the Gels plugin in Image J. Lysosome-enriched fractions were extracted according to the Folch procedure (Folch et al., 1957). The desalted Folch upper phases (aqueous phases), containing gangliosides, were analyzed by liquid chromatography coupled with high resolution mass spectrometry (LC-HRMS) in the negative ionization mode to detect deprotonated singly [M-H]- and doubly charged ions [M-2H]2-. Data were treated and analyzed as described previously (Seyer et al., 2016). The relative amount of each lipid was quantified as the area of its chromatographic peak, and it was normalized to the concentration of proteins in each lysosome-enriched fraction.

Hexosaminidase A activity

Hexosaminidase A activity was monitored as previously described (Niemir et al., 2018). Fifty mg of cortex were ground in 300 µl of 0.1 M citrate phosphate buffer, pH 4.5 and homogenates were lysed by three cycles of rapid freezing and thawing, followed by centrifugation at 4°C for 5 min at 10 000 g. The protein content of each supernatant was determined using the BCA kit. In a black 96-well plate with clear bottom, 10 µl of 1/10-diluted supernatant was added to 50 µl of the fluorimetric β-hexosaminidase A substrate [4-methylumbelliferyl-7–(6-sulfo-2-acetamido-2-deoxy-β-D-glucopyranoside (Calbiochem) at 1 mM in 0.1 M citrate phosphate buffer at pH 4.5]. The samples were incubated for 1 h at 37°C with gentle agitation and enzymatic reactions were stopped by adding 200 µl of a 1M glycine buffer, pH 10. The released fluorescence was read on a CytoFluor 4000 fluorimeter (PerSeptive Biosystems), excitation: 360 ± 40 nm, emission: 460 ± 40 nm. The data obtained were compared with the fluorescence of a 4-methyl-umbelliferone standard (10 nmol/well). Enzyme activity was expressed as nmol/h/mg cell protein.

Cellular reprogramming, characterization, and differentiation of iPS cells

Fibroblasts were reprogrammed into iPS cells by transient expression of OCT3/4, L-MYC, SOX2, KLF4, and LYN28 using episomal vectors as previously described (Okita et al., 2011). iPS cells were cultured on Geltrex matrix in complete E8 medium (Life technologies). We assessed the pluripotency of the iPS cells by differentiating them into embryoid bodies (EBs). iPSc clones were collected by collagenase treatment and resuspended in E8 medium without FGF2. Two weeks later, EBs were plated on polyornithine (20 µg/ml) and laminin (10 µg/ml)-coated cover slips and incubated for seven additional days. EBs were assessed for markers of the three germ layers: ectoderm (Nestin, Millipore), mesoderm (α-smooth muscle actin, Abcam), and endoderm (α-fetoprotein, Cell Signalling). iPS cells and EBS were also analyzed by real-time qPCR assays (TaqMan hPSC Scorecard Panel; Life Technologies) to confirm expression of pluripotency markers. iPS cells were differentiated into brain organoids following the protocol previously described (Pasca et al., 2015). After 90 days *in vitro*, organoids were fixed in 4% paraformaldehyde for 24 h, cryoconserved, and stored at -80°C. Organoid slices (12 µm) were cut on a cryostat (LEICA_CM3050S) and processed for immunostaining as described for the mouse brain slices. Images were obtained using a Leica SP-8 confocal microscope with a 60x objective (NA 1.4). Quantification of ganglioside accumulation was performed as for the mouse brain sections.

Primary cultures of neurons

Mouse primary cultures of cortical neurons were prepared as described (Branchu et al., 2017). When needed, neurons were treated with miglustat (Tocris) from the second day in culture. Medium was changed every three days. Vectors expressing miRNAs to downregulate GM3 synthase (GM3S), Neu1 and clathrin heavy chain (CHC) expression were produced using the Block-it kit (Life Technologies). The miRNA sequences were: ATGTACAGGAGCCAGACTCCAGTTTTGGCCACTGACTGACTGGAGTCTCTCCTGTACAT (miRNA GM3S-1), ATAACAGAGCCATAGCCGTCTGTTTTGGCCACTGACTGACAGACGGCTGGCTCTGTTAT (miRNA GM3S-2), TCTACAGAGCCGATCTGCTTCGTTTTGGCCACTGACTGACGAAGCAGAGGCTCTGTAGA (miRNA Neu1-1), CTACGATGAAGGCTGTAGAGGGTTTTGGCCACTGACTGACCCTCTACACTTCATCGTAG (miRNA Neu1-2), TATCAATGATTACCACCTGGGGTTTTGGCCACTGACTGACCCCAGGTGAATCATTGATA (miRNA CHC-1) and AATATTAGCTGACAGCATGGCGTTTTGGCCACTGACTGACGCCATGCTCAGCTAATATT (miRNA CHC-2). Neurons were transfected with vectors expressing the miRNA and GFP using the Neon transfection system (Life Technologies) with the following parameters: 1500V, 10ms, and 3 pulses. The efficiency of the miRNA sequences was validated by transfecting NIH-3T3 cells and performing quantitative RT-PCR using a LightCycler 480 apparatus (Roche) following the manufacturer's instructions.

For each replicate of lipidomic analysis, 10^6 neurons were grown in 100 cm^2 plate for six days *in vitro*. Neurons were washed twice in PBS, scraped and centrifuged at 5000g for 5 minutes. Dry pellet was kept at -80°C until samples were processed for lipidomic as detailed for lysosome-enriched fractions. The relative amount of GM2 was quantified as the area of its chromatographic peak, and it was normalized to the concentration of proteins in each pellet.

Immunostaining was performed after six days of culture *in vitro*, as previously described (Murmu et al., 2011), and images acquired using an Apotome2 microscope (Zeiss) with an objective Plan-Apochromat 63x

(N.A. 1.4), or with a Leica SP-8 confocal microscope. Ganglioside levels were quantified as the mean grey value using ImageJ. Colocalization of ganglioside staining with lysosomes was quantified using ImageJ on images of cultured neurons that were randomly chosen. First, we created a mask corresponding to Lamp1 staining using automatic threshold in Image J. The mask was copied to the corresponding fluorescence image of ganglioside. We quantified the total intensity of ganglioside fluorescence in the lysosome mask, and expressed it as the percentage of total ganglioside fluorescence in every neuron. A similar method was used to quantify the amount of clathrin colocalized with GM2 immunostaining. Live imaging of lysosome was performed on neurons transfected with a vector allowing expression of Lamp1-mCherry (Addgene, #45147) using a Yokogawa Confocal Spinning Disk module associated to a Leica DMi8 inverted microscope. For Cathepsin B activity assays, neurons were incubated with Magic Red™ Cathepsin B Assay Kit (1X according to manufacturer's instructions, ImmunoChemistry Technologies, #938) for 1h. Then, cells were fixed and stained with anti-α-tubulin and Alexa Fluor 488 secondary antibody. The average cathepsin B activity was monitored as the mean value of fluorescence measured with an automated ArrayScan XTI apparatus (Thermo-Fisher), using the general intensity measurement protocol. More than 1,500 cells were analysed per condition.

Neuronal death was induced by the addition of 200 µM glutamate (Sigma-Aldrich) in culture medium. To quantify neuronal death, 30 hours after glutamate treatment all neurons were labeled with 100 nM Cell tracker Deep Red (Life Technologies) and dead cells were labeled by propidium iodide (5 µM). The number of neurons positive for propidium iodide was quantified with an automated ArrayScan XTI apparatus using the compartmental analysis protocol.

Yeast two hybrid screen

The yeast two-hybrid screen was performed by Hybrigenics (Paris, France) with the 1943-2443 domain of human spatacsin as bait using an adult human cDNA brain library.

Coimmunoprecipitation

Hela cells were transfected with the Neon transfection system to express GFP-spatacsin (aa1943-2443). Cells were lysed in 100mM NaCl, 20mM Tris HCl, pH7.4, 1mM EDTA, 0.1% NP40 and complete inhibitor protease (Roche). GFP-spatacsin was immunoprecipitated using GFP-Trap beads (ChromoTek). Lysates and immunoprecipitates were separated by SDS-PAGE and immunoblotted onto nitrocellulose membranes. Western immunoblotting was performed with rabbit anti-GFP (Abcam) and mouse anti Dynamin (BD Biosciences) antibodies, and revealed using the West dura chemiluminescent substrate (Pierce).

Analysis of zebrafish model

Assessment of GM2 ganglioside levels in zebrafish larvae was performed at 48 hpf by whole-mount *in vivo* immunohistochemistry using 48 hpf embryos fixed in 4% paraformaldehyde in PBS for 2 h at room temperature. Embryos were washed 3 times in PBS-0.1% Triton X-100 (PBST). Embryos were blocked for 1 h in 5% normal goat serum in PBS containing 1% DMSO and 1% Triton X-100 (PBDT), then incubated overnight at 4 °C in PBDT containing the anti-GM2 primary antibody. After 4 washes in PBST, embryos were incubated with secondary antibody coupled to Alexa-488 (Thermo Fisher), overnight at room temperature in PBDT. Before observation, embryos were washed 3 times in PSBT and mounted in a drop of Fluoromount™ Aqueous Mounting Medium (Sigma Aldrich). Whole-mount embryos were imaged on a confocal microscope (Leica SP8, 40X, NA 0.8). Larvae were oriented in the same position for image capture to minimize potential biases in quantification. Image stacks were collected with a step-size of 0.35µm. Using ImageJ software, the maximum intensity projections of z-stacks were used for quantification of fluorescence in the telencephalon. Mean and variance of the fluorescence intensity were quantified for each morphant in a square of 100 pixels per 100 pixels. To quantify motor activity, we monitored the touch-evoked escape response at 48 hpf in larvae with no obvious developmental abnormalities as previously described (Martin et al., 2012). Images were acquired at 350 images per sec. Tracking of the touch evoked escape response was performed as previously described using the Image J manual tracking plugin (Fontaine et al., 2013).

Supplemental References

Branchu, J., Boutry, M., Sourd, L., Depp, M., Leone, C., Corriger, A., Vallucci, M., Esteves, T., Matusiak, R., Dumont, M., *et al.* (2017). Loss of spatacsin function alters lysosomal lipid clearance leading to upper and lower motor neuron degeneration. Neurobiol Dis 102, 21-37.

Dobrenis, K., Joseph, A., and Rattazzi, M.C. (1992). Neuronal lysosomal enzyme replacement using fragment C of tetanus toxin. Proc Natl Acad Sci U S A 89, 2297-2301.

Esteves, T., Durr, A., Mundwiller, E., Loureiro, J.L., Boutry, M., Gonzalez, M.A., Gauthier, J., El-Hachimi, K.H., Depienne, C., Muriel, M.P., *et al.* (2014). Loss of association of REEP2 with membranes leads to hereditary spastic paraplegia. Am J Hum Genet 94, 268-277.

Folch, J., Lees, M., and Sloane Stanley, G.H. (1957). A simple method for the isolation and purification of total lipides from animal tissues. J Biol Chem 226, 497-509.

Fontaine, R., Affaticati, P., Yamamoto, K., Jolly, C., Bureau, C., Baloche, S., Gonnet, F., Vernier, P., Dufour, S., and Pasqualini, C. (2013). Dopamine inhibits reproduction in female zebrafish (Danio rerio) via three pituitary D2 receptor subtypes. Endocrinology 154, 807-818.

Graham, J.M. (2001). Isolation of lysosomes from tissues and cells by differential and density gradient centrifugation. Curr Protoc Cell Biol Chapter 3, Unit 3 6.

Martin, E., Yanicostas, C., Rastetter, A., Naini, S.M., Maouedj, A., Kabashi, E., Rivaud-Pechoux, S., Brice, A., Stevanin, G., and Soussi-Yanicostas, N. (2012). Spatacsin and spastizin act in the same pathway required for proper spinal motor neuron axon outgrowth in zebrafish. Neurobiol Dis 48, 299-308.

Murmu, R.P., Martin, E., Rastetter, A., Esteves, T., Muriel, M.P., El Hachimi, K.H., Denora, P.S., Dauphin, A., Fernandez, J.C., Duyckaerts, C., *et al.* (2011). Cellular distribution and subcellular localization of spatacsin and spastizin, two proteins involved in hereditary spastic paraplegia. Mol Cell Neurosci 47, 191-202.

Natoli, E.J., Jr., Livingston, P.O., Pukel, C.S., Lloyd, K.O., Wiegandt, H., Szalay, J., Oettgen, H.F., and Old, L.J. (1986). A murine monoclonal antibody detecting N-acetyl- and N-glycolyl-GM2: characterization of cell surface reactivity. Cancer Res 46, 4116-4120.

Niemir, N., Rouviere, L., Besse, A., Vanier, M.T., Dmytrus, J., Marais, T., Astord, S., Puech, J.P., Panasyuk, G., Cooper, J.D., *et al.* (2018). Intravenous administration of scAAV9-Hexb normalizes lifespan and prevents pathology in Sandhoff disease mice. Hum Mol Genet 27, 954-968.

Okita, K., Matsumura, Y., Sato, Y., Okada, A., Morizane, A., Okamoto, S., Hong, H., Nakagawa, M., Tanabe, K., Tezuka, K., *et al.* (2011). A more efficient method to generate integration-free human iPS cells. Nature methods 8, 409-412.

Pasca, A.M., Sloan, S.A., Clarke, L.E., Tian, Y., Makinson, C.D., Huber, N., Kim, C.H., Park, J.Y., O'Rourke, N.A., Nguyen, K.D., *et al.* (2015). Functional cortical neurons and astrocytes from human pluripotent stem cells in 3D culture. Nature methods 12, 671-678.

Seyer, A., Boudah, S., Broudin, S., Junot, C., and Colsch, B. (2016). Annotation of the human cerebrospinal fluid lipidome using high resolution mass spectrometry and a dedicated data processing workflow. Metabolomics 12, 91.